

In situ Observation by X-Ray Diffraction of Structural Changes in Y-TZP

Yukishige Kitano and Yuuji Mori

Toray Research Center, Inc., Otsu, Shiga 520, Japan

Takaki Masaki

Toray Industries, Inc., Otsu, Shiga 520, Japan

ABSTRACT

The tetragonal-to-monoclinic phase transformation on ground and polished surfaces of tetragonal zirconia polycrystals containing 2.5 mol% yttria was studied using an in situ X-ray diffraction technique. The amount of monoclinic phase caused by thermal-stress-induced transformation reached a maximum value at 250°C, and the thermally stressed specimens exhibited much greater (111) peak intensity than that of (111), as similarly observed in specimens associated with mechanical stresses.

INTRODUCTION

Polycrystalline yttria-stabilized tetragonal zirconia (Y-TZP) exhibits both high strength and high fracture toughness qualities derived from the transformation of metastable tetragonal (t) to monoclinic (m) zirconia when stresses are imposed near the stress field of a crack tip. The tetragonal-to-monoclinic (t-to-m) transformation by not only mechanical but also thermal stress. Experimental observations of such processes as low-temperature ageing (1,2), annealing under humid conditions (3), and creep tests (4) have shown that transformation by thermal stress is induced at approximately 200° to 300°C.

For the present study, in situ X-ray diffraction was conducted on the ground and polished surfaces of 2.5 mol% Y-TZP during thermally induced stress to observe structural changes and determine the direct martensitic temperature. The relation between changes in intensity caused by thermal stress and those caused by mechanical stress is discussed.

EXPERIMENTAL PROCEDURE

Polycrystalline ZrO_2 materials stabilized with 2.5 mol% Y_2O_3 containing 0.5 mol% Al_2O_3 were prepared by the method previously reported (5). Test specimens were prepared by both pressureless sintering and hot isostatic pressing (HIP). The powder was first isostatically pressed at 200 MPa, then heated gradually from room temperature to 900°C at a rate of 50°C/h, and finally held at 1450°C for 2 h.

Hot isostatic pressing was conducted on samples pressed at 200 MPa and presintered for 2 h at 1400°C so as to obtain material with a density no less than 97% of theoretical. An unencapsulated sample was raised from room temperature to the maximum temperature at a rate of 700°C/h in an argon atmosphere; the gas pressure was adjusted to rise slowly, reaching 200 MPa at the maximum temperature. The sample was then treated at 1400°C for 1.5 h. The specimens obtained were ground with a 400-grit diamond wheel and then with 10- μm diamond paste to an optical finish. The surfaces of these specimens were polished further with 5- and then 3- μm diamond paste.

X-ray diffraction measurements were performed* using graphite monochromated $\text{CuK}\alpha$ radiation with an electronic furnace on a goniometer under dried nitrogen gas atmosphere. The XRD was accomplished by operating at 50 kV to 200 mA in step scan mode with a 0.01 2θ step and a counting time of 1 s/step, over a 2θ range of 27° to 40°; this range covers the monoclinic {111}, tetragonal {111}, and {002} peaks. The m-phase contents and intensity ratios of m(111)/m(111) and t(002)/t(200) were estimated from the relative areas under the {111} and {002} profiles using the method of Garvie and Nicholson (6).

RESULTS AND DISCUSSION

Figure 1 shows the XRD profiles for the ground surfaces after the specimens were heated to 800°C, then cooled to 200°C, and finally held 5 to 10 h. The m-phase contents and X-ray intensity ratios of the (002)/(200) tetragonal and (111)/(111) monoclinic peaks are summarized in Table 1. The m-phase, which appears on the ground surfaces at room temperature, almost disappears when the sample was heated to 800°C. When the sample was cooled from 800° to 200°C, the m-phase increased gradually with increased heating time.

The reversal of the intensity ratio of the (002)/(200) tetragonal peaks, which might be interpreted as domain switching, was also observed on the present specimens (7-9). Figure 1 shows that this reversal of tetragonal peaks was stable during heat treatment.

Figures 2 and 3 show the XRD profiles for the polished surfaces of the HIPed and pressureless sintered specimens, respectively. Figures 2(a) and 3(a) show the profiles of the specimens measured immediately after heating to 200°, 225°, 250°, 275°,

* Model RU-200B, Rigaku Corp., Tokyo, Japan.

and 300°C. Figures 2(b) and 3(b) show the profiles of the specimens measured after holding for 1 h at the setting temperatures.

The m-phase contents and $m(111)/m(\bar{1}\bar{1}\bar{1})$ intensity ratios of these specimens are summarized in Table 2.

The m-phase content of the HIPed specimens, measured after holding for 1 h at the setting temperatures, increased with increased heating temperature, reaching a maximum value at 250°C, then decreased with increased heating temperature from 275° to 300°C. Less m-phase was measured immediately after heating to the setting temperature than after holding for 1 h, although the amount reached a maximum at 250°C.

The pressureless sintered specimens, on the contrary, exhibited comparatively the same amounts of m-phase in all ranges of the heating temperature from 200° to 300°C, even just after heating to the setting temperatures.

This difference in m-phase content between the HIPed and the pressureless sintered specimens can be attributed to differences in grain size and density. The grain size and density of the HIPed specimens were 0.4 to 0.5 μm and 6.07 $\text{mg}\cdot\text{m}^{-3}$, respectively; those specimens thus were slightly finer and denser than the pressureless sintered specimens (0.5 μm and 6.00 $\text{mg}\cdot\text{m}^{-3}$, respectively), due to the lower sintering temperature of 1400°C. The t-to-m transformation of the HIPed specimens therefore is slower than that of the pressureless sintered specimens (2).

The {111} monoclinic peaks of the specimens showed much greater disparity between the (111) and $(\bar{1}\bar{1}\bar{1})$ peaks than that observed in diffraction studies of powders or of randomly transformed precipitates or grains within a matrix. These observations indicate a marked preference for the formation of the (111) orientation, as previously observed in specimens stressed during mechanical grinding or fracture (8).

REFERENCES

1. Kobayashi, K., Kuwashima, H., and Masaki, T., Phase change and mechanical properties of $\text{ZrO}_2\text{-Y}_2\text{O}_3$ solid electrolyte after ageing. *Solid State Ionics*, 1981, 3/4, 489-93.
2. Masaki, T., Mechanical properties of Y-PSZ after ageing at low temperature. *Int. J. High Technology Ceramics*, 1986, 2, 85-98.
3. Sato, T. and Shimada, M., Transformation of yttria-doped tetragonal ZrO_2 polycrystals by annealing in water. *J. Am. Ceram. Soc.*, 1985, 68, 356-59.
4. Matsui, M., Soma, T., and Oda, I., Stress induced transformation and plastic deformation for Y_2O_3 -containing tetragonal zirconia polycrystals. 1986, 69, 198-202.
5. Masaki, T. and Shinjo, K., Mechanical behavior of $\text{ZrO}_2\text{-Y}_2\text{O}_3$ ceramics formed by hot isostatic pressing. In *Advances in Ceramics*, Volume 24, Science and Technology of Zirconia II, ed. S. Somiya, N. Yamamoto, and H. Yanagida, The American Ceramic Society, Inc., Westerville, OH, 1988, pp. 709-20.
6. Garvie, R. C. and Nicholson, P. S., Phase analysis in zirconia systems. *J. Am. Ceram. Soc.*, 1972, 55, 303-05.

7. Virkar, A.V. and Matsumoto, R.L.K., Ferroelastic domain switching as a toughening mechanism in tetragonal zirconia. J. Am. Ceram. Soc., 1986, 69, C-224-C-226.
8. Kitano, Y., Mori, Y., Ishitanani, A., and Masaki, T., Structural changes by mechanical and thermal stresses of 2.5-mol% - Y_2O_3 -stabilized tetragonal ZrO_2 polycrystals. J. Am. Ceram. Soc., 1988, 71, C-382-C-383.
9. Kitano, Y., Mori, Y., Ishitani, A., and Masaki, T., Structural changes by compressive stresses of 2.0-mol%-yttria-stabilized tetragonal zirconia polycrystals. J. Am. Ceram. Soc., 1989, 72, 854-55.

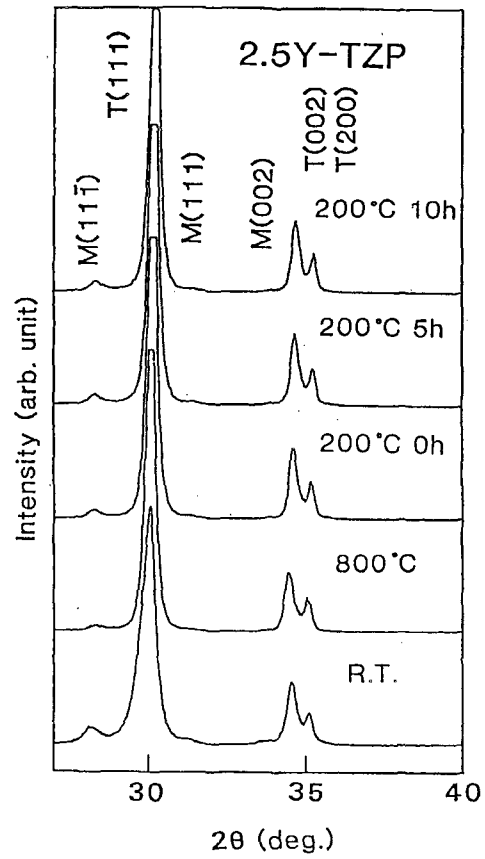


Figure 1. XRD profiles for the ground surfaces of 2.5Y-TZP after thermal stress.

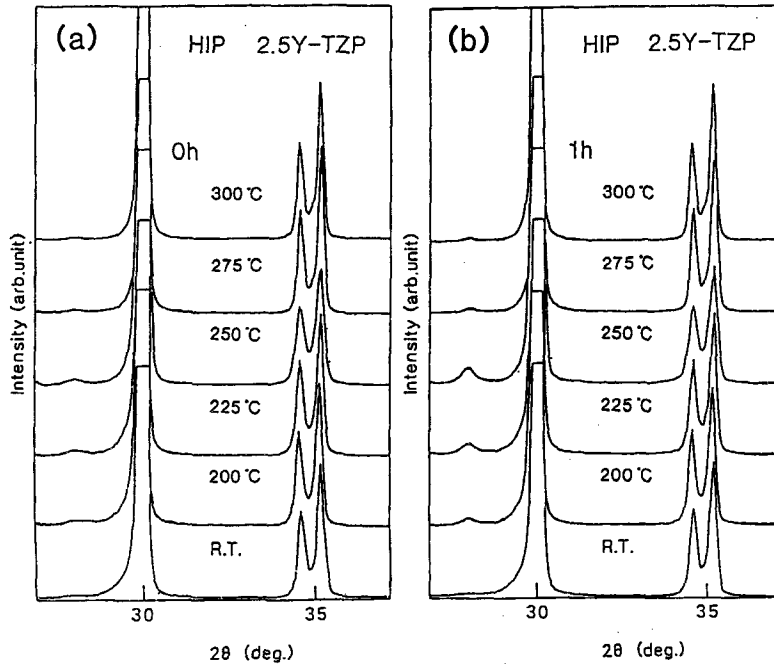


Figure 2. XRD profiles for the polished surfaces of hiped specimens (a) immediately after heating to and (b) after keeping for 1h at 200°, 225°, 250°, 275°, and 300°C.

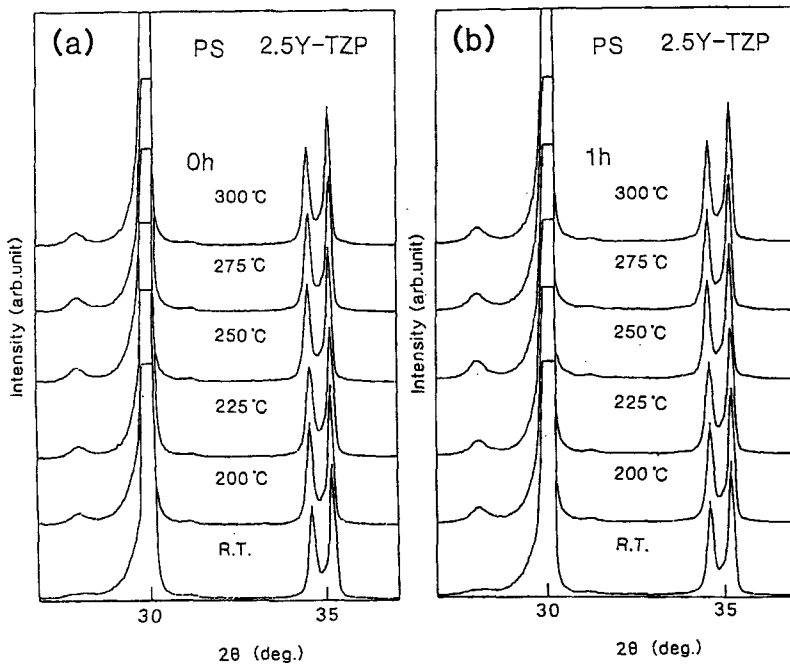


Figure 3. XRD profiles for the polished surfaces of pressureless sintered specimens (a) immediately after heating to and (b) after keeping for 1h at 200°, 225°, 250°, 275°, and 300°C.

TABLE 1
Effect of thermal-stresses on the m-phase contents
and XRD intensities

	M-phase contents (%)	Intensity ratio	
		T(002)/T(200)	M(111)/M(111)
ground surface			
R. T	5.0	4.2	0.3
800°C	1.5	3.1	5.8
200°C 0h	2.2	3.5	6.5
200°C 5h	2.7	3.3	7.4
200°C10h	3.0	3.3	8.1

TABLE 2
Effect of thermal-stresses on the m-phase contents
and XRD intensities

	HIP		PS	
	M-contents	N(111)/M(111)	M-contents	M(111)/M(111)
R. T	0.3	5.1	0.8	3.0
200°C 0h	0.6	6.3	1.8	8.5
1h	1.0	6.2	2.3	5.5
225°C 0h	0.7	8.0	2.0	9.3
1h	1.4	12.0	2.4	5.2
250°C 0h	1.2	7.2	2.2	6.3
1h	2.6	14.0	3.0	7.0
275°C 0h	0.5	5.3	2.2	9.0
1h	0.6	6.3	2.8	9.9
300°C 0h	0.3	2.7	1.8	4.4
1h	0.5	3.5	2.5	9.0